Effect of Ceramic Veneering on the Microstructure of Pre-sintered Cobalt-Chromium, Compared to Pre-sintered Zirconia and Conventional Cast Alloys

Elie E Daou[1,2*], Mutlu Özcan[3], Pascale Salameh[4-7], Ziad Salameh[1]

1. Department of Prosthodontics, Faculty of Dentistry, Lebanese university, Beirut, Lebanon
2. Department of Fixed Prosthodontics, Faculty of Dentistry, Saint Joseph university, Beirut, Lebanaon
3. Dental Materials Unit, Center for Dental and Oral Medicine, Clinic for Fixed and Removable Prosthodontics and Dental Materials Science, Zurich, Switzerland
4. Department of Public Health, Faculty of Pharmacy, Lebanese University, Beirut, Lebanon
5. Gilbert and Rose-Marie Chagoury School of Medicine, Lebanese American University, Beirut, Lebanon
6. Department of Primary Care and Population Health, University of Nicosia Medical School, Nicosia, Cyprus
7. Institut National de Santé Publique d'Épidémiologie Clinique et de Toxicologie-Liban (INSPECT-LB), Beirut, Lebanon

Article InfO	A B S T R A C T
Article type: Original Article	**Objectives:** We aimed to evaluate ceramic-alloy interface and emphasize the alteration of alloy microstructure after ceramic layering.
	Materials and Methods: Thirty-two discs made from a ceramic-alloy combination of pre-sintered cobalt-chromium (CoCr), cast CoCr, cast nickel-chromium (NiCr), or pre-sintered zirconia were prepared with eight discs in each group. Four specimens were examined as manufactured and four were ceramic-layered. Scanning electron microscopy (SEM), energy-dispersive X-ray spectroscopy (EDS), X-Ray diffractometer (XRD), and an atomic force microscope were used for analysis. Non-layered specimens received ceramic fire-heating without adding any ceramic. Alloy microstructure was compared before and after ceramic veneering or heating within the same group. Mean differences in grain size and surface roughness were compared among groups. P<0.05 was considered significant.
Article History: Received: 10 Aug 2023 Accepted: 25 Feb 2024 Published: 11 Aug 2024	
	Results: SEM showed a close bonding interface between alloys and ceramics. EDX demonstrated differences compared to the manufacturer's composition. Ceramic-layering reduced grain size for both milled alloys (P<0.05), whereas grain size increased in cast groups (P=0.011). Heat treatment did the same for the CoCr groups (P=0.013). Ceramic veneering increased the surface roughness of the cast CoCr (Gi) (P=0.029) and NiCr (Wi) (P=0.005) groups, whereas zirconia roughness average (Ra) showed a slight decrease (P=0.282). XRD showed no differences among zirconia, NiCr, and milled CoCr groups before and after veneering. Crystallite size differed between monoclinic and tetragonal phases in zirconia.
* Corresponding author: Department of Prosthodontics, Faculty of Dentistry, Lebanese University, Beirut, Lebanon; Department of Fixed Prosthodontics, Faculty of Dentistry, Saint Joseph University, Beirut, Lebanon Email: edaou@ul.edu.lb elie.daou2@usj.edu.lb	**Conclusion:** The study highlights that ceramic-layering induces significant microstructural changes in alloys, enhancing bonding potential and mechanical stability. Pre-sintered materials show a fine homogeneous surface, optimizing ceramic adherence and potentially improving clinical outcomes.
	Keywords: Dental Materials; Materials Testing; Zirconium

INTRODUCTION

Cobalt-chromium (CoCr), considered more biocompatible, has replaced the commonly used nickel-chromium (NiCr) as a substructure for dental ceramics. The International Organization for Standardization does not require any specific composition of the cobalt-based alloys used for metal-ceramic restorations. The mass percentage varies among the three main constituents: Co as the

main constituent, Cr not less than 25% (m/m), molybdenum not less than 4% (m/m), and Co+Ni+Cr not less than 85% (m/m).[1,2]

The strength of the ceramic bond to zirconia and base metal alloys has ranged between 9.4 MPa and 95 MPa.[3,4] The mechanical, chemical, Van Der Waals, and compressive forces may control the metal-porcelain liaison.[5] The chemical bond may be crucial in the adhesion process. It may be made possible by an electron structure continuity across the metal-metal oxide interface and the metal oxide-porcelain interface through metallic, ionic, and covalent bonds.[6] These bonds may result from the formation of specific reactive oxides in the most superficial layer of cast alloys[7].

The interface preparations before porcelain-layering, as well as the reactions that promote adhesion, are essential in porcelain fused to metal (PFM) restorations.[8,9] The nature of the interface between novel alloys and porcelain is still not fully understood.[10] Chemical reactions were cited to occur,[11] with time-dependent diffusion processes.[12] However, wet, thick layers of porcelain may induce changes in the surface grains of partially-sintered materials.[13] In prosthetic dentistry, studies have principally evaluated the fit of the prostheses and the adherence of the ceramic to the substructure.[14,15] Few studies have focused on the evaluation of internal porosity, surface roughness, and chemical properties.[16,17] Furthermore, analyses of the properties of alloy structures made from different manufacturing techniques are scarce.[16,18] Large differences in the structure of the specimens may be anticipated, resulting from complete melting in the casting technique and the full sintering of frameworks milled in the green state. These variations in microstructures may also influence the characteristics of the metal-porcelain interface. Chipping and delamination may result from interfacial characterization and reduce the longevity of restorations in the intra-oral environment.

Microstructural properties may have clinical outcomes. Mechanical properties (such as fatigue resistance), electrochemical characteristics, and other properties may be altered by microstructural changes.[16] This trial attempted to analyze the microstructure of alloys and evaluate the quality of the ceramic-porcelain interface. The aim was to focus on the metallurgical characterization of pre-sintered CoCr and zirconia and evaluate the interfacial modification after the veneering process. The first null hypothesis was that there would be significant structural dissimilarities among the groups issued from different manufacturing techniques. The second null hypothesis was that conventional porcelain firings would not affect the underlying microstructure of the tested alloys.

MATERIALS AND METHODS

The study protocol received IRB approval from the University of Lebanese University (CUMED/ D127/142018). Thirty-two discs, each with a 15mm diameter and 2mm thickness, were created from disc-shaped 3D models (STL files) using Ceramill Mind software (Amann Girrbach AG, Austria). These specimens were then assigned to the appropriate material blanks according to the software (Table 1).

The two groups (N=16) were milled using a Ceramill Motion 2 milling machine (Amann Girrbach AG). The pre-sintered CoCr (CS) group (N=8) was pre-sintered with CAD-CAM CoCr (Ceramill Sintron, Amann Girrbach AG), and the pre-sintered Zr (CZ) group (N=8) was pre-sintered employing CAD-CAM zirconia (Ceramill Zi, Amann Girrbach AG). The discs were cut from the blanks, then sintered: the CS group in a Ceramill Argotherm furnace

Table 1. Material, fabrication methods, and composition used in each experimental group (N=8)

Group	Generic name	Manufacturer	System	Ceramic coating
Ceramill Sintron	Pre-sintered CoCr	Amann Girrbach AG	Soft milled CAD-CAM	Vita M13 Vita Zahnfabrik, Bad Saeckingen
Girobond nb	Cast CoCr	Amann Girrbach AG	Lost wax/ cast	Vita M13 Vita Zahnfabrik, Bad Saeckingen
Wiron 99	Cast NiCr	Bego	Lost wax/ cast	Vita M13 Vita Zahnfabrik, Bad Saeckingen
Ceramill Zi	Pre-sintered Zr	Amann Girrbach AG	Soft milled CAD-CAM	Vita M13 Vita Zahnfabrik, Bad Saeckingen

and the CZ group in a Ceramill Therm furnace. The other two groups (N=16) were milled from Ceramill wax blocks, with the cast NiCr Wi group (N=8) cast in NiCr alloy (Wiron 99, Bego GmbH, Canada) and the cast CoCr (Gi) group (N=8) cast in CoCr alloy (Girobond nb, Amann Girrbach AG) according to the manufacturer's instructions. The sample size was calculated based on a prior study using the same methodology, where a sample size of 3 specimens was considered sufficient. Groups of 8 specimens were used in the current study to enhance statistical power, with 4 specimens in each subgroup.

Only one surface of each specimen was polished using silicon carbide grinding papers with abrading grains of 1,000 and 4,000, successively (Carbimet PSA, Buehler, UK), and a rotating grinding disc apparatus (Motopol 8, Buehler, UK).[19] Specimens were then cleaned in an ultrasonic water bath for 5 minutes.[16]

Ceramic-alloy interface analysis: Only one surface of the specimens was ceramic layered with a 2mm thickness, following the manufacturer's instructions,[14] using ceramic layering (Vita M13 and M9, Vita Zahnfabrik, Bad Saeckingen, Germany). Vita M13 was used for CoCr and NiCr, and Vita M9 for zirconia. The specimens were sectioned longitudinally after being embedded in auto-polymerized acrylic resin (Alike, GC America, Switzerland) with a diamond saw (NTi Flex, KaVo Kerr, USA) and ground finished to 400 grit silicon carbide abrasive (Dura-green Wheels, Shofu Dental Asia, Singapore). They were polished using a diamond paste (Diamond Twist SCL, Premier Dental, USA), following 6, 3, and 0.25 μm felt disc sequence (Flexi Buff, Cosmedent, USA), under water coolant irrigation.[20] Scanning electron microscopy (SEM) (AIS2100C, Seron technologies, Korea) was used to analyze the ceramic-alloy interface of each group. A line profile covering the ceramic-interfacial zone-alloy was drawn, allowing line scan measurements. At each point, the intensity profile of major elements was analyzed. The accelerating voltage was set at 12 kV with a magnification of ×1000. Energy-dispersive X-Ray analysis (EDX) was performed with an EDAX Apollo detector coupled to the SEM.

Alloy grains size measurement: To realize a mapping of the atomic-scale topography of disc surfaces and to determine the surface roughness of materials, an atomic force microscope (AFM) was used (Agilent 5420, Measurement by contact mode). Grain sizes were measured based on AFM images using the Image J software (National Institutes of Health). The surface roughness of materials was measured based on AFM images using the formula

$$Ra = \frac{1}{n} \sum_{i=1}^{n} yi \,.[21]$$

Measurements were performed on images taken on discs as they were being manufactured and after ceramic veneering.

To better explore the first results obtained from CoCr groups, non-layered CoCr discs (Si and Gi) were submitted to all conventional porcelain firing steps without veneering on any disc surface. This step aimed to discern if microstructural changes reported for these two alloys were related to ceramic layering or heat treatment.

Alloys crystal phases determination: An X-Ray diffractometer (XRD) was used for phase identification and unit cell dimensions. Before ceramic veneering, the disc surfaces were evaluated to determine the crystal phases of the alloys (CS and CZ groups as milled and Wi and Gi groups as cast) using an XRD machine (D8 Advance, Bruker, USA) with an accelerating voltage of 40 kV, a beam current of 40 mA, a 2θ angle scan range of 30-110∘, a scanning speed of 0.02∘/sec, a sampling pitch of 0.02∘, and a preset time of 1 sec. The XRD graphs were used to calculate the crystallite size of the alloys using the Debye-Scherrer equation Ʈ= ƙλ/ ß cos(ó)[.22] This step was performed to ensure that changes at the materials interface following the porcelain build-up were not associated with transformations due to exposure to room temperature humidity before porcelain veneering, especially for the pre-sintered alloys.[10]

Statistical analysis: The General Linear Model was employed to assess mean differences in grain size and surface roughness among groups. The mean difference was significant at the 0.05 level.

RESULTS

The SEM images showed an intimate bonding interface between alloys and porcelain

veneering for the four tested groups. There were some voids within the ceramic. Milled alloys showed a more homogenous structure, compared to the cast alloys. Line scans illustrated element variations in each specimen between porcelain and alloys (Figure 1). These line scan curves were incorporated into the SEM images of the EDS spectra sites for instruction purposes.

Higher oxidation was found in the cast groups than in the milled group. The EDX quantification showed element variations in CoCr alloys after each treatment, compared to the manufacturer's declared composition (Table 2). Differences were reported between materials and after treatment sequences (Table 3).

Ceramic layering significantly reduced grain sizes in both milled alloys ($P<0.05$), whereas grain sizes significantly increased in the cast alloys (P=0.011). Heat treatment did

the same in the Gi and CS groups (P=0.013) (Table 4) (Figure 2). Pairwise comparison showed finer grains in the milled groups, with a significant difference between the CZ and CS groups (P=0.010). This study confirmed the homogenous surface of the zirconia alloy with finer grains than the other three tested groups (Table 5). A significant difference in roughness average (Ra) values was found between the CoCr groups (P=0.007). Ceramic veneering significantly increased the surface roughness of the Gi (P=0.029) and NiCr (P=0.005) groups. On the other hand, the Ra values of zirconia material showed a slight decrease (P=0.282) (Table 6).

The XRD analysis showed no differences among the CZ, Wi, and CS groups before and after porcelain veneering. There was a difference in the Gi group. There was a change in the peaks after heat treatment without ceramic in the Gi group. Fire heating induced differentiation of crystalline structure in the Gi group (Figure 3). The ceramic application produced a crystallite size change in the Gi group. This was also found between heat treatment and ceramic application in this group. No similar changes were reported in the CS and Wi groups after any of the treatments. The crystallite size also differed between monoclinic and tetragonal phases in zirconia (Table 7).

Table 2. Energy dispersive X-Ray (EDX) analysis of the three materials with and without ceramic (numbers indicate weight percentage)

EDX	Disc	Disc+ceramic
Ceramill Sintron	6.17	17.12
Ceramill Zi	11.92	12.88
Wiron99	10.18	20.08
Girobond nb	7.23	24.47
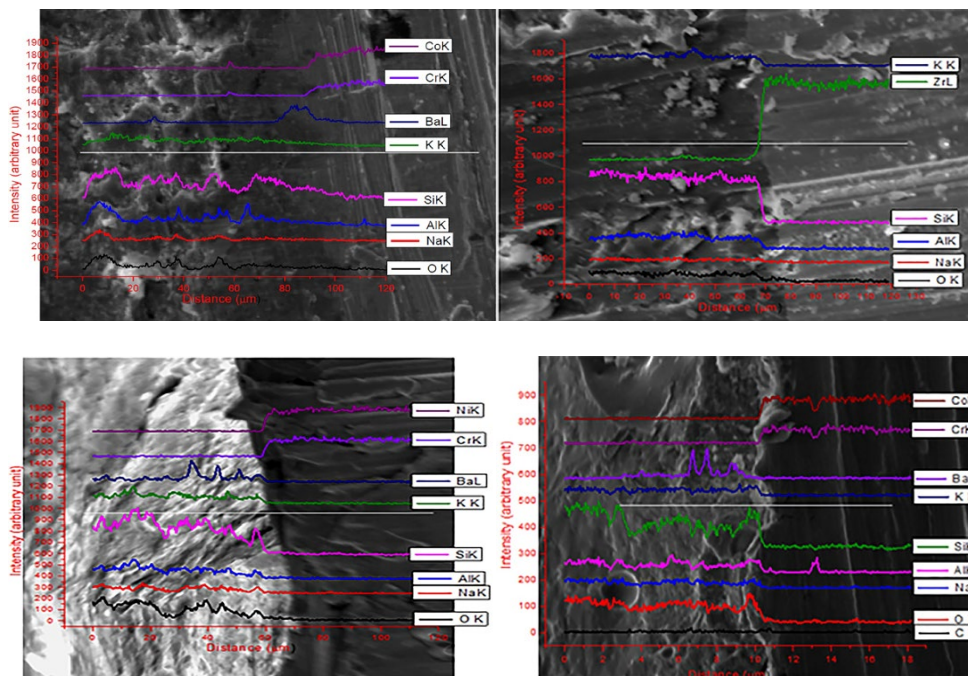
Fig. 1. Line scan analysis for Ceramill Sintron specimen, Ceramill Zi specimen, Wiron 99 specimen, and Girobond nb specimen from left to right, respectively (V:12, Mag:×1000).

Table 3. Energy dispersive X-Ray analysis quantification (weight percentage) of CoCr alloys after each treatment, compared to the manufacturer's declared composition (Total in each row=100)

|	Element	Co	Cr	Mo	W	Si	Ce	Fe	Nb	Mn	C	O	AL	Na	K	Ba
Manufacturer's Composition	**CS**	66	28	5	5	<1	-	<1	-	<1	-	-	-	-	-	
	Gi	62	25	5	5	1	<1	<1	<1	-	-	-	-	-	-	-
EDX Quantification	**CS**	50.29	27.26	5.23	-	1.5	-	-	-	-	9.55	6.17	-	-	-	
	Gi	56.94	24.14	-	9.36	4.94	-	-	-	-	2.84	1.78	-	-	-	-
	CS+Ceramic	28.26	15.57	2.81	-	17.72	-	-	-	-	8.6	17.12	5.67	-	-	
	Gi+Ceramic	19.54	8.76	-	-	21	-	-	-	-	7.41	24.47	6.49	4,89	3.77	3.66

CS: Ceramill Sintron
GI: Girobond nb
EDX: Energy-dispersive x-ray analysis

Table 4. The mean grain size measured from atomic force microscope images (µm)

| Material	As manufactured	After ceramic layering	After heat treatment	P Before/after ceramic layering	P Before/after Heat treatment
Ceramill Sintron	0.14	0.09	0.11	0.016	0.013
Girobond nb	0.11	0.15	0.09	0.011	0.013
Wiron 99	0.08	0.15		>0.05	
Ceramill Zi	0.11	0.07		0.016	
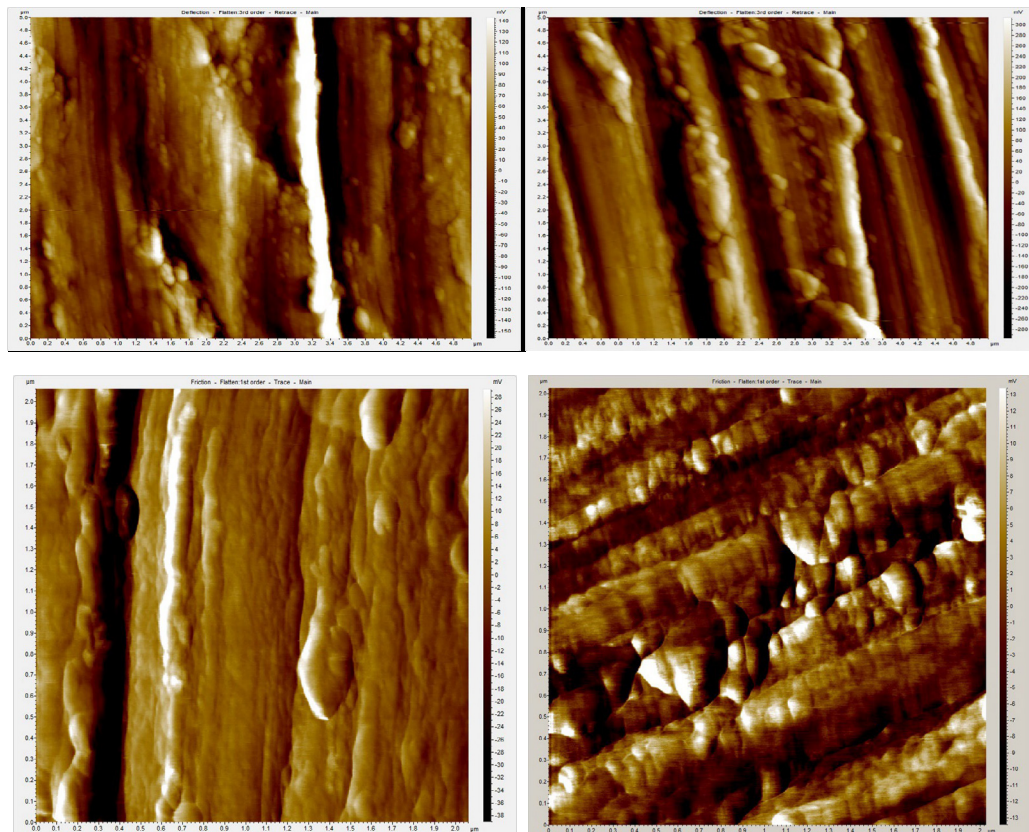
Fig. 2. Atomic force microscope images from top to bottom: Ceramill Sintron, Girobond nb, Ceramill Zi, and Wiron 99

Table 5. Pairwise comparison for grain size and surface roughness

(I) Material	(J) Material	Grains size Mean Difference (I-J)	P	Surface Roughness Mean Difference (I-J)	P
Ceramill Sintron	Ceramill Zi	0.02	0.08	-0.006	0.157
Ceramill Sintron	Girobond nb	-0.01	0.35	-0.01	0.007
Ceramill Sintron	Wiron 99	0.003	0.84	-0.004	0.950
Ceramill Zi	Girobond nb	-0.04	0.01	-0.004	0.723
Ceramill Zi	Wiron 99	-0.02	0.12	0.002	1.000

Table 6. Disc surface roughness (μm) of materials before and after ceramic layering

Surface roughness	Ceramill Sintron	Ceramill Zi	Wiron 99	Girobond nb
As manufactured	0.012±0.006	0.021±0.003	0.009±0.004	0.012±0.006
After ceramic veneering	0.016±0.004	0.020±0.003	0.027±0.005	0.038±0.009
P	0.167	0.282	0.005	0.029
Fire heating	0.028±0.003			0.003±0.008
P	<0.001			<0.001
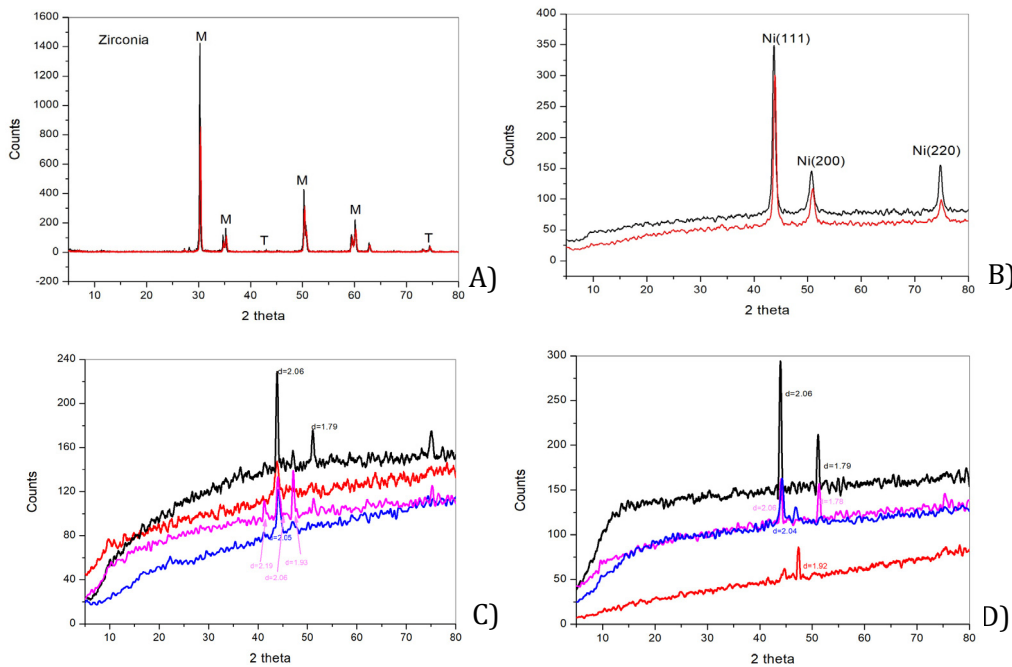
Fig. 3. Comparison of X-Ray diffraction as cast or milled (black) after heat treatment (blue), with opaque layer (pink), and with ceramic (red). A) Ceramill Zi, B) Wiron 99, C) Girobond nb, and D) Ceramill Sintron.

Table 7. The mean crystallite size calculated from X-Ray diffraction for each material in each preparation phase (nm). Size differences found between groups are shown with the same letter.

Material	As cast/milled	With ceramic	Heat treatment
Ceramill Sintron	1.328	1.330	1.427
Girobond nb	1.731[a]	0.654[a,b]	1.753[b]
Wiron99	1.057	1.057	
Ceramill Zi	Monoclinic (with/without ceramic)	Tetragonal (with/without ceramic)	
	1.096[c]	1.779[c]	

DISCUSSION

The current study evaluated the effect of ceramic veneering on the microstructure of pre-sintered CoCr and zirconia. Ceramic layering or fire heating induced a statistically relevant change in the grain size values in all the tested materials. At the crystallite level, ceramic layering affected the CoCr microstructure in the milled and cast groups, whereas the heat treatment process only changed the crystallite structure of the Gi. Additionally, there were significant differences between Gi and CZ groups after each treatment application. Therefore, the null hypotheses were partially rejected, which is in contrast with the findings of other studies, where heat treatment did not demonstrate significant alterations in the microstructure of cast alloys.[12]

A random distribution of small spherical pores was found in all groups, but they were more pronounced in the cast groups. This confirmed the findings of other studies, in which X-ray radiography revealed porosity in the cast group but not in the milled or laser-sintered CoCr.[16] Non-homogeneous microstructure, solidification defects, and large grains in the Gi may reduce its mechanical properties and induce cracks within the alloy structure.[23] The results obtained in the present study confirmed that variations in the chemical composition and the microstructure of alloys might be found even in the as-cast condition.[24] Differences in the interfacial characterization of metallic elements in the metal-porcelain interface may result from differences in the microstructure of the materials.[16] The SEM images showed a more homogenous structure for the milled alloys. However, interfacial analyses of the CoCr alloys, cast or milled with porcelain, remain scarce in the dental literature.[25]

High oxidation was found in the EDX quantification, especially in the cast groups. The difference in shear bond strength mean values may result from oxide layer thickness, with a higher occurrence of metal-oxide-related failures reported for base metal PFM restorations.[26] The SEM investigations have proposed that these elements accumulate at the metal-ceramic interface to form an interfacial oxide layer.[27] The SEM exploration could not confirm these allegations in the present study. The SEM line scan only showed some oxygen on the surface of the cut specimens, and bulk oxidation could not be demonstrated. Boundary phase changes between metal and ceramic could not be proven by SEM and EDX, as reported by others.[28] This can be considered a limitation of this study, and how alloy surface is altered through preparation stages still needs to be fully explored.[29]

Ceramic application changed the grain size in all groups after each treatment. A net increase (30%) in grain size values was also found for the Gi group after ceramic layering, whereas a decrease of 17% was stated after fire heating (Table 4). Therefore, we concluded that the manufacturing process could significantly affect the alloy microstructure. On the other hand, the heat treatment induced grain size changes for both CoCr groups, which was an unexpected result for the CS group, not shown by crystallite size calculation. Further investigations are needed to confirm these findings. The CS group showed finer grains than Gi and Wi groups, without statistical relevance, which is an important finding for the CS group because dental materials should consist of small grains. Chipping failure that may occur in machined components with coarse grain structures may reduce the accuracy of the marginal fit of the restorations.[23] However, even if no correlation could be demonstrated between grain size and surface roughness, a net decrease in grain size after fire heating for the Gi was combined with a sharp decrease (75%) in surface roughness. Nevertheless, ceramic veneering and fire heating increased Ra values in all tested groups. These results may influence the bond strength between ceramic and different alloys.

The XRD results confirmed the variations before and after ceramic layering or heat treatment in the Gi group, which was not evident for CS, CZ, and Wi. This may be explained by the fact that the CS attained a stable and final crystal arrangement with minimum atomic energy upon sintering, whereas a phase transformation was well reported for the Gi after the fire heating or ceramic veneering (Figure 2). XRD analysis indicated that the microstructure of the cast and milled alloys consisted of a face-centered cubic (fcc) phase and was mainly composed of Co and Cr.[16,24][10] Amann Girrbach AG has declared that the crystal lattice structure of CS

is a mixture of cubic fcc and hexagonal (hcp). The exact percentage of the amounts has not been determined.[30] The XRD results confirmed that the main phases of both pre-sintered and cast CoCr were the ɣ-phase and ε-phases. The casting process uses a complete melting and overheating of the alloys, inducing higher peaks of ɣ- and ε-phases for the Gi, compared to the CS (Figure 3C-D). As an allotropic element, Co is characterized by an unstable fcc (ɣ-phase) structure. Pure Co moves from an fcc to an hcp (ε-phase) crystal structure with extremely slow cooling. The reported pure Co transformation temperature is 417°C, which can reach 900°C for Co alloys. Generally, the fcc phase is stable at a high temperature above 1120 K, while the hcp phase attains an equilibrium phase at room temperature.[23] The slow fcc↔hcp transformation at room temperature will preserve the unstable fcc structure.[18] A ɣ↔ε transformation was more apparent for the cast groups, resulting from slow cooling after the high-temperature melting of the alloys (Figures 3C and 3D). The ε-phase improves the strength and wear resistance of the CoCr alloys but can lead to poor ductility.[30]

It is important to note that when we compare the results of the crystallite size (Table 7) to those of the XRD (Figure 3), we can conclude that the heat treatment influenced only the crystal arrangement of the group Gi, but not its crystallite size. On the other hand, adding ceramic to a CoCr induced a change in the crystallite size in this group of the Gi, proving that an interaction occurred between the two materials. Conversely, ceramic layering had no major influence on the crystallite size in the groups CS and Wi. The crystallite size differed also between monoclinic and tetragonal phases in group CZ, with no influence of ceramic veneering within the same phase.

Y-TZP, a metal-oxide, may develop a chemical bonding comparable to that of the metal-porcelain interface.[31] Authors agree that analytical techniques with low resolution did not allow the recording of relevant differences in chemical elements' composition at the zirconia-ceramic interface.[32] The SEM analysis was unable to prove a zirconia dissolution in the feldspathic glass (Figure 1B), which can be considered a limitation of the present study. The authors could not prove a clear chemical interaction,[11] comparable to the veneering ceramic attachment to the metal core. Nevertheless, high-resolution interfacial ultra-morphologic characterization may have exposed a tight interface between zirconia and its veneering ceramic.[11] Interfacial flaws may cause stress concentrations and ceramic debonding.[33] A recent study, using μRaman microscopy, did not report any diffusion in the zirconia core, but only minor element movements in the layering porcelain.[32]

Lower t-phase peaks were reported in the current study after ceramic layering, combined with some $t_è m$ phase transformation (Figure 3A). Before the veneering procedure, Y-TZP ceramics may consist only of the t-phase.[13] Liquid presence in the veneering porcelain may initiate a $t_è m$ transformation. This $t_è m$ phase transformation may result from veneer diffusion into the zirconia surface during firing processes, with high-stress concentrations at the interface.[32,34] Even if the zirconia core has been reported to stay intact,[32] a localized zirconia volume increase at the interface may influence the veneer stability.[13] The adherence of porcelain to zirconia core and its stability in the oral environment needs further investigation.

CONCLUSIONS

Within the limitations of the present study, the following conclusions can be drawn:

- Group CS possesses an intimate interface with ceramic, which can ameliorate the bonding between the two materials.
- Unlike group Gi, which exhibited phase transformation after fire-heating without ceramic, the group CS group attained a stable and final crystal arrangement upon sintering. This stable microstructure in group CS reduces deformation in complex FDP frameworks after ceramic veneering.
- Pre-sintered materials showed fine, homogeneous surfaces that can enhance bonding with layering ceramic. Further investigations are required to fully understand the ceramic-pre-sintered alloys interface. The fine grains in group CS can theoretically improve framework adaptation.

CONFLICT OF INTEREST STATEMENT

Non declared.

REFERENCES

1. ISO 6871-1: 1994, Dental base metal casting alloys-Part 1: Cobalt-based alloys, ISO, Geneva, 1998, pp. 1-6.

2. DIN E. 22674 (2006): Dentistry–Metallic materials for fixed and removable restorations and appliances. DIN-Taschenbuch.;267(1):524-53.

3. Anusavice KJ, Ringle RD, Fairhurst CW. Bonding mechanism evidence in a ceramic--nonprecious alloy system. J Biomed Mater Res. 1977 Sep;11(5):701-9.

4. Guess PC, Kulis A, Witkowski S, Wolkewitz M, Zhang Y, Strub JR. Shear bond strengths between different zirconia cores and veneering ceramics and their susceptibility to thermocycling. Dent Mater. 2008 Nov;24(11):1556-67.

5. Li KC, Ting S, Prior DJ, Waddell JN, Swain MV. Microstructural analysis of Co-Cr dental alloy at the metal-porcelain interface: A pilot study. NZ Dent. J. 2014 Dec;1(110):138-42.

6. Takaichi A, Suyalatu, Nakamoto T, Joko N, Nomura N, Tsutsumi Y, et al. Microstructures and mechanical properties of Co-29Cr-6Mo alloy fabricated by selective laser melting process for dental applications. J Mech Behav Biomed Mater. 2013 May;21:67-76.

7. Podrez-Radziszewska M, Haimann K, Dudziński W, Morawska-Sołtysik M. Characteristic of intermetallic phases in cast dental CoCrMo alloy. Archives of foundry engineering. 2010;10(3):51-6.

8. Hallmann L, Ulmer P, Reusser E, Louvel M, Hämmerle CH. Effect of dopants and sintering temperature on microstructure and low temperature degradation of dental Y-TZP-zirconia. J Eur Ceram Soc. 2012 Dec 1;32(16):4091-104.

9. Tholey MJ, Swain MV, Thiel N. Thermal gradients and residual stresses in veneered Y-TZP frameworks. Dent Mater. 2011 Nov;27(11):1102-10.

10. Tholey MJ, Berthold C, Swain MV, Thiel N. XRD2 micro-diffraction analysis of the interface between Y-TZP and veneering porcelain: role of application methods. Dent Mater. 2010 Jun;26(6):545-52.

11. Inokoshi M, Yoshihara K, Nagaoka N, Nakanishi M, De Munck J, Minakuchi S, et al. Structural and Chemical Analysis of the Zirconia-Veneering Ceramic Interface. J Dent Res. 2016 Jan;95(1):102-9.

12. Ozkomur A, Ucar Y, Ekren O, Arai Shinkai RS, Teixeira ER. Characterization of the interface between cast-to Co-Cr implant cylinders and cast Co-Cr alloys. J Prosthet Dent. 2016 May;115(5):592-600.

13. Hallmann L, Ulmer P, Wille S, Kern M. Effect of differences in coefficient of thermal expansion of veneer and Y-TZP ceramics on interface phase transformation. J Prosthet Dent. 2014 Sep;112(3):591-9.

14. Daou EE, Özcan M, Salameh P, Al-Haj Husain N, Salameh Z. Comparison of Adhesion of a Novel Pre-sintered Cobalt-Chromium to Pre-sintered Zirconia and Cast Nickel-Chromium. J Contemp Dent Pract. 2018 Jul 1;19(7):816-823.

15. Daou EE, Ounsi H, Özcan M, Al-Haj Husain N, Salameh Z. Marginal and internal fit of pre-sintered Co-Cr and zirconia 3-unit fixed dental prostheses as measured using microcomputed tomography. J Prosthet Dent. 2018 Sep;120(3):409-414.

16. Al Jabbari YS, Koutsoukis T, Barmpagadaki X, Zinelis S. Metallurgical and interfacial characterization of PFM Co-Cr dental alloys fabricated via casting, milling or selective laser melting. Dent Mater. 2014 Apr;30(4):e79-88.

17. Revilla-León M, Al-Haj Husain N, Methani MM, Özcan M. Chemical composition, surface roughness, and ceramic bond strength of additively manufactured cobalt-chromium dental alloys. J Prosthet Dent. 2021 May;125(5):825-831.

18. Al Jabbari YS. Physico-mechanical properties and prosthodontic applications of Co-Cr dental alloys: a review of the literature. J Adv Prosthodont. 2014 Apr;6(2):138-45.

19. Rosentritt M. A focus on zirconia : an in-vitro lifetime prediction of zirconia dental restorations. PhD thesis Universiteit Amsterdam; 2008.

20. Vásquez VZ, Ozcan M, Kimpara ET. Evaluation of interface characterization and adhesion of glass ceramics to commercially pure titanium and gold alloy after thermal- and mechanical-loading. Dent Mater. 2009 Feb;25(2):221-31.

21. International Organization for Standardization. 4287-Geometrical Product Specifications (GPS)-Surface Texture: Profile Method-Terms, Definitions and Surface Texture Parameters; International Organization for Standardization: Geneva, Switzerland, 1997

22. MacDonald MJ, Vorberger J, Gamboa EJ, Drake RP, Glenzer SH, Fletcher LB. Calculation of Debye-Scherrer diffraction patterns from highly stressed polycrystalline materials. J. Appl. Phys..

2016 Jun 7;119(21).

23. Lu Y, Wu S, Gan Y, Li J, Zhao C, Zhuo D, et al. Investigation on the microstructure, mechanical property and corrosion behavior of the selective laser melted CoCrW alloy for dental application. Mater Sci Eng C Mater Biol Appl. 2015 Apr;49:517-525.

24. Takaichi A, Suyalatu, Nakamoto T, Joko N, Nomura N, Tsutsumi Y, et al. Microstructures and mechanical properties of Co-29Cr-6Mo alloy fabricated by selective laser melting process for dental applications. J Mech Behav Biomed Mater. 2013 May;21:67-76.

25. Culha O, Zor M, Gungor MA, Arman YU, Toparli M. Evaluating the bond strength of opaque material on porcelain fused to metal restorations (PFM) alloys by scratch test method. Materials & Design. 2009 Sep 1;30(8):3225-8.

26. Venkatachalam B, Goldstein GR, Pines MS, Hittelman EL. Ceramic pressed to metal versus feldspathic porcelain fused to metal: a comparative study of bond strength. Int J Prosthodont. 2009 Jan-Feb;22(1):94-100.

27. Hong JM, Razzoog ME, Lang BR. The effect of recasting on the oxidation layer of a palladium-silver porcelain alloy. J Prosthet Dent. 1988 Apr;59(4):420-5.

28. Wu Y, Moser JB, Jameson LM, Malone WF. The effect of oxidation heat treatment of porcelain bond strength in selected base metal alloys. J Prosthet Dent. 1991 Oct;66(4):439-44.

29. Johnson T, van Noort R, Stokes CW. Surface analysis of porcelain fused to metal systems. Dent Mater. 2006 Apr;22(4):330-7.

30. Hong MH, Lee DH, Hanawa T, Kwon TY. Comparison of microstructures and mechanical properties of 3 cobalt-chromium alloys fabricated with soft metal milling technology. J Prosthet Dent. 2022 Mar;127(3):489-496.

31. Kappert H, Eichner K. In: Eichner K, ed Dental materials and their processing. 5th ed, Huthig, Heidelberg. 2005;1988;1:77-86

32. Durand JC, Jacquot B, Salehi H, Fages M, Margerit J, Cuisinier FJ. Confocal Raman microscopic analysis of the zirconia/feldspathic ceramic interface. Dent Mater. 2012 Jun;28(6):661-71.

33. Tsuruki J, Kono H, Okuda Y, Noda M, Arikawa H, Kanie T,Ban S. Factors affecting on the bond strength of dental zirconia to veneering porcelains. Key Eng Mater 2013; 529-530: 507-511.

34. Durand JC, Jacquot B, Salehi H, Margerit J, Cuisinier FJ. Confocal Raman microscopy and SEM/EDS investigations of the interface between the zirconia core and veneering ceramic: the influence of a liner and regeneration firing. J Mater Sci Mater Med. 2012 Jun;23(6):1343-53.